Dimesogenic compounds with an electron-attracting terminal group

Dong Won Lee; Jung-Il Jin; M. Laguerre; M. F. Achard; F. Hardouin

PLEASE SCROLL DOWN FOR ARTICLE

Dimesogenic compounds with an electron-attracting terminal group

DONG WON LEE, JUNG-IL JIN

Center for Electro- and Photoresponsive Molecules and Department of Chemistry,
Korea University, Seoul 136-701, Korea

M. LAGUERRE

Institut Européen de Chimie et Biologie,
Ecole Polytechnique-Université Bordeaux I-Université Bordeaux II,
Avenue Pey-Berland, 33402 Talence, France

M. F. ACHARD and F. HARDOUIN*

Centre de Recherche Paul Pascal, Université Bordeaux I, Av. A. Schweitzer,
33600 Pessac, France

Non-symmetric dimesogens composed of a classical aromatic mesogenic unit linked to a cholesteryl moiety by a flexible spacer form several types of smectic periodicities: one is connected to the cholesteryl length and the other to the length of the associated dimesogens. In some peculiar cases, anomalies of periodicity resulting from the competition between these incommensurate lengths are observed through the occurrence of two-dimensional modulated phases or incommensurate low ordered smectic phases (S_{ic})†. As part of our continuing effort to understand the influence on the smectic arrangement of the molecular parameters of such non-symmetric dimesogens, new homologues with a cholesteryl unit linked by a penta-methylene spacer to an aromatic mesogenic moiety bearing different electron attracting terminal groups have been prepared. For these compounds, only the periodicity resulting from the associated dimesogens is observed. Nevertheless, an incommensurate smectic phase can be induced by mixing one of these compounds with another appropriate dimesogen. Molecular mechanics calculations suggest that the origin of the different smectic structures is strongly connected to the repartition of electrostatic potential along the dimesogen.

1. Introduction

The smectic phase behaviour of non-symmetric dimesogens, in which two different mesogenic groups are linked by a flexible spacer, appears rather intriguing. Indeed, within the same series, certain homologues form an intercalated smectic phase in which the layer spacing is close to half the molecular length, while other homologues exhibit smectic phases in which the periodicity is larger than the molecular length [1]. In all the examples, the nature of the smectic phase formed has been found to depend on the relative length of the spacer and the terminal chains [1–3]. Between these two regimes, depending on the dimesogen series, the smectic phase vanishes [4] or anomalies of periodicity are revealed through the occurrence of two-dimensional modulated phases (antiphase $S_{\tilde{A}}$ [3, 5, 6] or ribbon phase $S_{\tilde{C}}$ [6, 7]) and in some rare cases of the incommensurate fluid smectic phase S_{ic} [6, 8].

For several years, we have focused on dimesogens composed of a classical mesogenic unit with two aromatic rings linked to a cholesteryl moiety by a spacer

*Author for correspondence; e-mail: F.HARDOUIN
@presidence-bx1.u-bordeaux.fr

† The nomenclature used by the authors in this and earlier papers is based on the smectic periodicity rather than on the tilted or non-tilted nature of the phase. This system has been preserved with its use of S for smectic rather than the conventional Sm employed in the Journal (Editor).

[2, 6, 8–11]. These compounds, denoted as KI-*n(m)* (where *n* and *m* refer to the number of methylene groups in the spacer and the length of the terminal chain, respectively), display two types of smectic packing: they are found to form smectic phases with a periodicity close to the dimesogen length, labelled the 'S$_{q1}$' phase, and/or a smectic phase with a layer spacing lower than half the molecular length, labelled the 'S$_{q3}$' phase. The dependence of the smectic layering on the length of the terminal alkyl chain, when the spacer length is kept constant (*n* = 5), shows that the early members (*m* = 2, 3, 4) exhibit intercalated structures, while the longer homologues (*m* = 5, 6, 10) show a 'dimer' modulation [10]. A reversed evolution of the layer spacing versus the spacer length is observed (the aliphatic tail is now kept constant at *m* = 4): short spacers correspond to a periodicity close to the dimesogen length (S$_{q1}$ phase) and long spacers to S$_{q3}$ phases [2].

However, contrary to other non-symmetric dimesogens, the cholesteryl compounds do not respond to the frustration induced by two incommensurate lengths by destroying the smectic phase, but by inducing smectic phases with anomalies of periodicity. For example, KI-5(4) constitutes an intermediate regime in which the system hesitates between the two periodicities and develops commensurate S$_{q1}$ and S$_{q3}$ phases, incommensurate S$_{ic}$ and two-dimensional fluid smectic S$_{\tilde{c}}$ phases [6, 8]. As for rod-like polar smectics [12], a two-dimensional modulated phase in which the two density modulations are not collinear, constitutes an escape to the incommensurability [6]. In the incommensurate smectic phases [6], the two incommensurate wavevectors *q*1 and *q*3 are collinear and the two competing periodicities coexist at long range.

As part of our continuing effort to understand the structure–property relationships for the cholesteryl-based dimesogens, we have now replaced the alkyl chain of the reference compound KI-5(4) by different terminal groups X, as shown in the structure below:
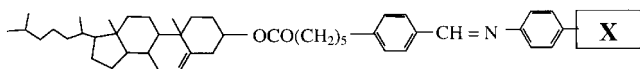
A minor modification consists of putting a weakly electron donating group X = −OC$_3$H$_7$ in place of the −C$_4$H$_9$ tail. As other possible variations of the KI-5(4) formula, we have introduced different electron attracting groups: X = −COCH$_3$, −CH=CH−COO−C$_2$H$_5$ (KII-5), −CN and −NO$_2$. Note that we have chosen the cyano and nitro groups since anomalies of periodicity have been observed mainly in polar calamitic mesogens [13] (even though an incommensurate fluid smectic phase has never been revealed in such systems), and also recently in a series of polar non-symmetric dimesogens [3].

2. Experimental
2.1. *Synthesis*
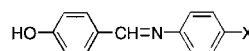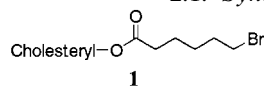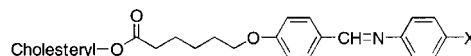
X = -OPr **(5)**: KI-5OC$_3$H$_7$
X = -COCH$_3$ **(6)**: KI-5COCH$_3$
X = -CN **(7)**: KI-5CN
X = -NO$_2$ **(8)**: KI-5NO$_2$

Since the synthetic procedure was same for all of the compounds, a representative preparative method is given in detail only for compound **5**.

Compound **1** and mesogens **2**–**5** which contain the Schiff's base part were prepared by the method described in our earlier paper [8]. The final compound **5** was synthesized by reacting compound **1** (1.0 eq, 5.64 g, 10 mmol) with **2** (1.2 eq, 3.06 g, 12 mmol). They were dissolved in 150 ml of *N,N*-dimethylformamide containing 2.12 g Na$_2$CO$_3$ (2.0 eq, 20 mmol) and 4 Å molecular sieves. After the mixture had been stirred at 120°C for 12 h under a dry nitrogen atmosphere, it was cooled to room temperature, and slowly poured into a large excess of distilled water to remove Na$_2$CO$_3$. The precipitate was collected on a filter, then dissolved in methylene chloride and insoluble material removed by filtration. After the solvent was evaporated, crude compound **5** was purified by recrystallization from methylene chloride/ethanol (1:3 by volume), and washed thoroughly with dimethyl sulfoxide, ethanol, and finally acetone. The product was dried at 40°C in a vacuum oven. The yield was 81.2% (5.99 g).

5 (KI5-OC$_3$H$_7$). ^{1}H NMR (300 MHz, CDCl$_3$, ppm): 0.67–2.01 (m, 52H, −C<u>H</u>−, −C<u>H</u>$_2$−, C<u>H</u>$_3$), 2.30–2.33 (m, 4H, −COC<u>H</u>$_2$−, =CH−C<u>H</u>$_2$−), 3.93 (t, 2H, −OC<u>H</u>$_2$CH$_2$−), *J* = 6.6 Hz, 4.02 (t, 2H, −OC<u>H</u>$_2$CH$_2$−), *J* = 6.3 Hz, 4.56–4.62 (m, 1H, −OC<u>H</u>−), 5.38 (m, 1H, −C=C<u>H</u>−), 6.91 (d, 2H, −N=CH−Ar−<u>H</u>(*meta*)), *J* = 8.8 Hz, 6.95 (d, 2H, −CH=N−Ar−<u>H</u>(*meta*)), *J* = 8.8 Hz, 7.19 (d, 2H, −N=CH−Ar−<u>H</u>(*ortho*)), *J* = 8.8 Hz, 7.81 (d, 2H, −CH=N−Ar−<u>H</u>(*meta*)), *J* = 8.8 Hz, 8.39 (s, 1H, −C<u>H</u>=N−). FTIR (KBr, cm^{-1}): 3045 (Ar C−H stretching), 2915, 2830 (aliphatic C−H stretching), 1730 (ester C=O stretching), 1612, 1574, 1511 (Ar C=C stretching), 1248,

1173 (ester C—O stretching), 1108 (C—O—C stretching). Elemental analysis: calc. for $C_{49}H_{71}NO_4$: C 79.74, H 9.70, N 1.90; found: C 79.76, H 9.70, N 1.91%.

6 (KI5-COCH₃). ¹H NMR (300 MHz, CDCl₃, ppm): 0.69–2.03 (m, 47H, —C$\underline{H}$—, C$\underline{H}_2$—, C$\underline{H}_3$), 2.30–2.36 (m, 4H, —COC$\underline{H}_2$—, =CH—C$\underline{H}_2$—), 2.62 (s, 3H, —COC$\underline{H}_3$—), 4.04 (t, 2H, —OC$\underline{H}_2$CH₂—), $J = 6.0$ Hz, 4.58–4.60 (m, 1H, —OC$\underline{H}$—), 5.39 (m, 1H, —C=C$\underline{H}$—), 6.98 (d, 2H, —N=CH—Ar—$\underline{H}$(*meta*)), $J = 8.8$ Hz, 7.21 (d, 2H, —N=CH—Ar—$\underline{H}$(*ortho*)), $J = 8.8$ Hz, 7.83 (d, 2H, —CH=N—Ar—$\underline{H}$(*ortho*)), $J = 8.8$ Hz, 7.99 (d, 2H, —CH=N—Ar—$\underline{H}$(*meta*)), $J = 8.8$ Hz, 8.35 (s, 1H, —C$\underline{H}$=N—). FTIR (KBr, cm⁻¹): 3039 (Ar C—H stretching), 2907, 2815 (aliphatic C—H stretching), 1732 (ester C=O stretching), 1674 (aryl ketone C=O stretching), 1626, 1583, 1512 (Ar C=C stretching), 1256, 1165 (ester C—O stretching), 1075 (C—O—C stretching). Elemental analysis: calc. for $C_{48}H_{67}NO_4$: C 79.84, H 9.35, N 1.94; found: C 79.83, H 9.37, N 1.97%.

7 (KI5-CN). ¹H NMR (300 MHz, CDCl₃, ppm): 0.67–2.02 (m, 47H, —C$\underline{H}$—, C$\underline{H}_2$—, C$\underline{H}_3$), 2.17–2.36 (m, 4H, —COC$\underline{H}_2$—, =CH—C$\underline{H}_2$—), 4.04 (t, 2H, —OC$\underline{H}_2$CH₂—), $J = 6.3$ Hz, 4.57–4.63 (m, 1H, —OC$\underline{H}$—), 5.37 (m, 1H, —C=C$\underline{H}$—), 6.98 (d, 2H, —N=CH—Ar—$\underline{H}$(*meta*)), $J = 8.8$ Hz, 7.20 (d, 2H, —N=CH—Ar—$\underline{H}$(*ortho*)), $J = 8.8$ Hz, 7.66 (d, 2H, —CH=N—Ar—$\underline{H}$(*ortho*)), $J = 8.8$ Hz, 7.83 (d, 2H, —CH=N—Ar—$\underline{H}$(*meta*)), $J = 8.8$ Hz. FTIR (KBr, cm⁻¹): 3027 (Ar C—H stretching), 2909, 2828 (aliphatic C—H stretching), 2219 (CN stretching), 1731 (ester C=O stretching), 1628, 1587, 1512 (Ar C=C stretching), 1254, 1168 (ester C—O stretching), 1109 (C—O—C stretching). Elemental analysis: calc. for $C_{47}H_{64}N_2O_3$: C 80.07, H 9.15, N 3.97; found: C 80.10, H 9.44, N 3.81%.

8 (KI5-NO₂). ¹H NMR (300 MHz, CDCl₃, ppm): 0.67–2.03 (m, 47H, —C$\underline{H}$—, C$\underline{H}_2$—, C$\underline{H}_3$), 2.31–2.36 (m, 4H, —COC$\underline{H}_2$—, =CH—C$\underline{H}_2$—), 4.05 (t, 2H, —OC$\underline{H}_2$CH₂—), $J = 6.3$ Hz, 4.61–4.64 (m, 1H, —OC$\underline{H}$—), 5.37 (m, 1H, —C=C$\underline{H}$—), 7.09 (d, 2H, —N=CH—Ar—$\underline{H}$(*meta*)), $J = 8.8$ Hz, 7.23 (d, 2H, —N=CH—Ar—$\underline{H}$(*ortho*)), $J = 8.8$ Hz, 7.85 (d, 2H, —CH=N—Ar—$\underline{H}$(*ortho*)), $J = 8.8$ Hz, 8.27 (d, 2H, —CH=N—Ar—$\underline{H}$(*meta*)), $J = 8.8$ Hz, 8.34 (s, 1H, —C$\underline{H}$=N—). FTIR (KBr, cm⁻¹): 3080 (Ar C—H stretching), 2943, 2898 (aliphatic C—H stretching), 1732 (ester C=O stretching), 1340, 1600 (NO₂ stretching), 1625, 1581, 1508 (Ar C=C stretching), 1259, 1159 (ester C—O stretching), 1107 (C—O—C stretching). Elemental analysis: calc. for $C_{46}H_{64}N_2O_5$: C 76.21, H 8.90, N 3.86; found: C 76.26, H 8.88, N 3.84%.

2.2. *Experimental techniques*

The IR and ¹H NMR spectra of all intermediate and final compounds were recorded on a Bomem MB FTIR spectrophotometer and a Bruker AM300 spectrometer,

respectively. The thermal behaviour was investigated using a Perkin-Elmer DSC7 differential scanning calorimeter under a nitrogen atmosphere.

The optical textures of the mesophases were observed using a polarizing microscope (Leitz Diavert) equipped with a hot stage (FP-82HT) and an automatic controller (Mettler FP-90). When the sample formed a homeotropic texture on a regular glass slide, a rubbed polyimide substrate was used to observe the optical textures.

The mesophase structures were determined by X-ray diffraction experiments on powder and aligned samples. For the alignment procedure, the liquid crystal was first introduced by capillarity between two thin glass plates coated with polyimide and unidirectionally rubbed, and then subjected to a mechanical stress perpendicular to the rubbing direction. For the X-ray experiments, the CuK$_\alpha$ radiation from an 18 kW rotating anode X-ray generator (Rigaku-200) was selected by a flat (1 1 1) germanium monochromator. The scattered radiation was collected on a two dimensional detector (Imaging Plate system from Mar Research, Hamburg). The samples were placed in an oven, providing a temperature control of 0.1 K.

Computational methods used for molecular dynamics calculations and to determine electrostatic potential maps have been recently described [10].

3. Results and discussion
3.1. *Phase characterization*

The thermal transition behaviour of the compounds was examined by DSC and an initial characterization of the liquid crystalline phases was carried out by polarizing optical microscopy. X-ray diffraction experiments were performed to obtain structural identification. Results are summarized in tables 1 and 2.

3.2. *Mesomorphic properties*

In addition to the melting peak corresponding to a large enthalpy change, the materials show reversible thermal transitions indicating several mesophases. Compounds KI-5COCH₃, KI-5NO₂ and KI-5CN did not crystallize readily when the LC phase was cooled, but when heated again, they underwent a crystallization and melting process. The thermograms of KI-5CN are given as an example in figure 1.

On cooling from the isotropic liquid, all the members of the KI-5*X* series exhibit a cholesteric mesophase with characteristic Grandjean textures. A TGB phase was observed for KI5-COCH₃, KI-NO₂ and KI-5CN. As for KI-5(4); the assignment of the TGB phase was made from the observation of the characteristic vermis (no surface treatment) and Grandjean (rubbed polyimide) textures and by the existence of a resolution-limited X-ray peak at low angles. Without surface treatment, a

Table 1. Transition temperature (°C) and enthalpy, ΔH, data in brackets (kJ g^{-1}); mesophases in round brackets in a phase sequence indicate monotropic transitions.

Compound	Terminal group	Phase sequence
KI-5(4) reference compound	$-C_4H_9$	crystal $\xrightarrow{85\,°C}$ $S_{\dot{C}}$ $\xrightarrow{97\,°C}$ S_{q3} $\xrightarrow{141\,°C}$ S_{ic} $\xrightarrow{146\,°C}$ S_{q1} LT $\xrightarrow{152\,°C}$ S_{q1} HT $\xrightarrow{164\,°C}$ TGB $\xrightarrow{168\,°C}$ N* $\xrightarrow{192\,°C}$ I
KI-5OC$_3$H$_7$	$-OC_3H_7$	crystal $\xrightarrow[(38)]{117\,°C}$ S $\xrightarrow[(0.7)]{171\,°C}$ N* $\xrightarrow[(5)]{212\,°C}$ I
KI-5COCH$_3$	$-COCH_3$	crystal $\xrightarrow[(17)]{116\,°C}$ S $\xrightarrow{156\,°C}$ TGB $\xrightarrow[(03)]{160\,°C}$ N* $\xrightarrow[(5)]{213\,°C}$ I
KII-5 [2, 6]	$-CH=CH-$ $COO-C_2H_5$	crystal $\xrightarrow{139\,°C}$ S_{ic} $\xrightarrow{140\,°C}$ S_{q3} $\xrightarrow{206\,°C}$ N* $\xrightarrow{238\,°C}$ I
KI-5CN	$-CN$	crystal $\xrightarrow[(49)]{160\,°C}$ S $\xrightarrow{176\,°C}$ TGB $\xrightarrow[(0.4)]{178\,°C}$ N* $\xrightarrow[(5.5)]{216\,°C}$ I
KI-5NO$_2$	$-NO_2$	crystal $\xrightarrow[(52)]{178\,°C}$ N* $\xrightarrow[(4.4)]{208\,°C}$ I $(S_A) \xrightarrow[165\,°C]{}$ (TGB) $\xleftarrow[(0.5)]{167\,°C}$

Table 2. Wave vectors q (Å^{-1}) and layer spacing d (Å) in the smectic phases of the KI-5(X) compounds. L corresponds to the molecular length in the all-*trans*-conformation as estimated from molecular models. (—) indicates that the phase does not exist. $\langle\ \rangle$ indicates diffuse scattering.

	Smectic phase with only one wave vector $q1$ or $q3$				Smectic phase with the coexistence of the two wavevectors $q1$ and $q3$	
Compound	S_{q1}	S_{q3}	L	d/L	S_{ic} ($q1$ and $q3$ collinear)	modulated $S_{\dot{C}}$ ($q1$ and $q3$ not collinear)
KI-5(4)	0.153 Å^{-1} (41 Å)	0.313 Å^{-1} (20.1 Å)	44.5 Å	0.92 / 0.45	0.149 Å^{-1} (42.1 Å, $d/L=0.95$) 0.313 Å^{-1} (20.1 Å, $d/L=0.45$)	0.142 Å^{-1} 0.313 Å^{-1}
KI-5OC$_3$H$_7$	$\langle$ 0.154 Å$^{-1}\rangle$	0.317 Å^{-1} (19.8 Å)	44.4 Å	0.45	—	—
KI-5COCH$_3$	0.106–0.103 Å^{-1} (61 Å)	—	42.9 Å	1.42	—	—
KII-5 [2, 6]	—	0.302 Å^{-1} (20.8 Å)	47.9 Å	0.43	0.130–0.119 Å^{-1} (48.3–52.8 Å) $1.01 < d/L < 1.10$ 0.302 Å^{-1} (20.8 Å, $d/L=0.43$)	—
KI-5CN	0.096–0.094 Å^{-1} (65.4–66.8 Å)	—	42.7 Å	1.53–1.56	—	—
KI-5NO$_2$	0.101–0.099 Å^{-1} (62.2–63.4 Å)	—	42.1 Å	1.48–1.50	—	—

homeotropic texture spontaneously develops for the smectic phases of the KI-5*X* compounds which behave as uniaxial media. With a rubbed polyimide substrate, focal-conic textures are observed. Transitions involving S_{q1}, S_{q3} and S_{ic} phases show only subtle changes in the focal-conic textures, detectable during heating scans, but not evident from static photographs.

Through this first characterization, it was obvious that the dimesogens under study exhibit simpler phase sequences than the reference compound KI-5(4).
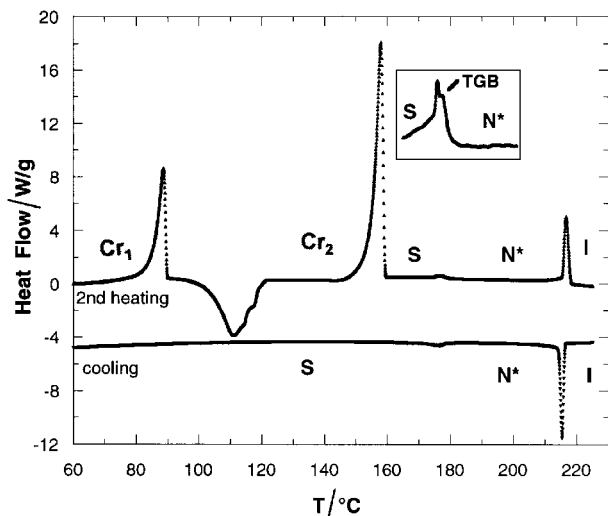
Figure 1.   DSC thermogram of compound KI-5CN on heating and cooling at $5°C\,min^{-1}$. Enlarged details are shown in the inset.

3.3 *Structural properties*

The smectic phases of the KI-5X compounds exhibit Bragg peaks in the low angle region and diffuse scattering in the wide angle domain which gives evidence of a liquid-like order within the layers.

As in our previous papers [2, 6, 8–11], we use a nomenclature based on the smectic periodicity rather than on the smectic C or smectic A nature of the phase. When the periodicity is related to the dimesogen length, the smectic phase is labelled 'S_{q1} phase' ($q1$ is the wave vector). When the layer spacing is lower than half the molecular length the phase is called 'S_{q3} phase' ($q3$ is the wave vector).

The KI-5(4) reference compound develops, in addition to the two types of smectic phase S_{q1} and S_{q3}, smectic phases in which the two wave vectors coexist, modulated $S_{\tilde{C}}$ (where $q1$ and $q3$ are not collinear) and an incommensurate fluid smectic S_{ic} where the wave vectors are collinear.

Let us now consider the effects of the modification to the formula of KI-5(4) on the structural properties of the smectic phases. X-ray data are summarized in table 2.

In KI-5OC$_3$H$_7$, we have introduced an oxygen atom in place of one CH$_2$ group. The phase sequence is dramatically reduced and only an S_{q3} phase remains. Nevertheless, the underlying periodicity $2\pi/q1$ is present as incommensurate fluctuations.

On the contrary, the smectic phases of KI-5COCH$_3$, KI-5CN and KI-5NO$_2$, are characterized by a layer spacing $d = 2\pi/q1$ larger than the dimesogen length with a d/L value lying between 1.4 and 1.6 (the molecular length L is estimated considering the molecule in the all-*trans*-conformation). Within our nomenclature, these

phases are S_{q1} phases. Nevertheless, we found a d/L ratio clearly higher than that for the other S_{q1} phases previously observed in the other cholesteryl dimesogens. However, up to now, we have no miscibility argument to differentiate these two types of S_{q1} phase.

Three smectic packings are thus observed in the cholesteryl-based dimesogens: an intercalated S_{q3} phase with $d/L = 0.45$ and two kinds of S_{q1} modulations either with a d/L ratio close to 1 or close to 1.5. This distinction reminds one of the different smectic A phases observed in polar smectics forming bimolecular associations [13]: monolayer smectic A1, partially bilayer smectic A$_d$ and bilayer smectic A2. It is likely that bimolecular antiparallel pairs also exist in all these non-symmetric dimesogens. Indeed molecular mechanics calculations showed that an antiparallel association of two adjacent cholesteryl dimesogens constitutes an energetically favourable configuration. In addition, the degree of overlapping of two molecules is the result of a subtle balance between electrostatic and van der Waals interactions [10]. According to these conclusions, one can easily imagine the occurrence of different layered structures resulting from a modification of the overlapping of antiparallel dimesogens. A change in the chemical formula will favour either the electrostatic or the van der Waals interactions and thus will modify the equilibrium between these two types of interactions. As a consequence, the pair conformation and the smectic layering order will be affected.

For all the KI-5X dimesogens, the negative potentials are strongly localized along the molecule and centred on the COO group of the cholesteryl part and on the oxygen of the spacer. Nevertheless, the repartition of the negative potential on the aromatic mesogenic unit strongly depends on the nature of the terminal group.

Let us first consider the KI-5(4) and KI-5OC$_3$H$_7$ molecules: the introduction of an oxygen atom leads to a symmetrical repartition of the negative potential (in blue) around the external aromatic ring (a), figure 2(a). As shown in table 2, this new repartition of the electrostatic potential does not affect the characteristic length connected with $q3$ but is sufficient to disfavour the periodicity connected with $q1$. In both cases, the overlapping obtained for antiparallel pairs corresponds to a regular alternation of the negative and positive potentials. The smectic order connected with $q3$ experimentally observed may result from these favourable interactions between the two kinds of mesogenic groups: the cholesteryl moiety can then impose a characteristic length relative to $q3$ since the aromatic mesogenic group is able to adapt to its layering size.

The case of the KI-5X compounds with an electron-attracting terminal group ($-$COCH$_3$, $-$CN or $-$NO$_2$) appears very different (figure 2(b)) since a strong
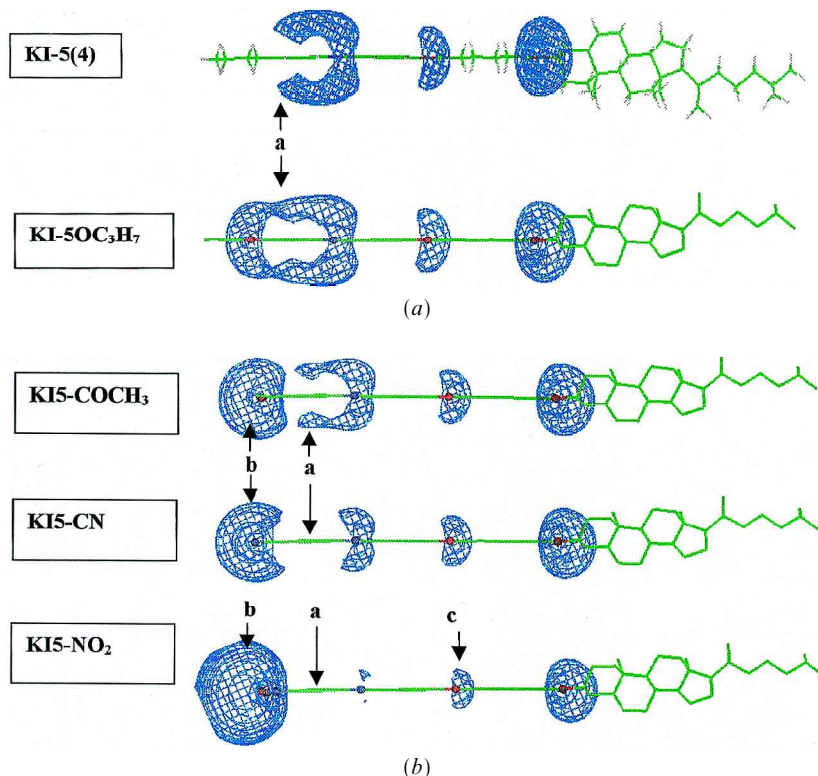
Figure 2(*a*).   Configuration of KI-5(4) and KI-5OC$_3$H$_7$ molecules resulting from Molecular Dynamics and electrostatic potential calculations (Blue contours at $-40\,\mathrm{kJ\,mol^{-1}}$). Molecules are drawn in stick representation with hydrogens omitted for clarity. O and N atoms are represented as red and blue balls respectively. *b*. Configuration of KI-5COCH$_3$, KI-5CN and KI-5NO$_2$ molecules.

negative potential lobe is localized at the extremity of the molecule (b), and the charge on the aromatic mesogenic unit (a) becomes very weak. It is worth noting that the $-NO_2$ group exerts its influence as far as the ether group of the spacer (c).

In these three systems, the constraint due to electro-static interactions between two adjacent dimesogens is strong and highly specific and this leads to the loss of the periodicity $2\pi/q3$ and to the development of the $2\pi/q1$ periodicity (table 2). For these three systems, the smectic layering is about 1.5 times the molecular length, since a complete overlapping of two dimesogens is not possible due to the negative terminal group.

A possible smectic organization of the KI-5CN dimesogens is given in figure 3. This representation is based on a favourable repartition of the electrostatic potential involving the perfect matching of the negative and positive parts. It appears rather realistic since the cholesteryl moiety can develop favourable interactions with either the spacer or the aromatic mesogens.

Results of molecular mechanics calculations involving 64 dimesogens (figure 4) confirm this arrangement and show that the cholesteryl moiety interacts much more favourably with the spacer, but much less with the aromatic mesogenic unit.

Finally, for the KII-5 dimesogen with a $-C{=}C-COO{-}C_2H_5$ terminal group (figure 5), an equilibrium between the different driving forces (the electrostatic and the van der Waals interactions) allows simultaneous observation of $q3$ and $q1$ wave vectors through the occurrence of an incommensurate low ordered smectic phase [6]. In this case, the periodicity connected to $q1$
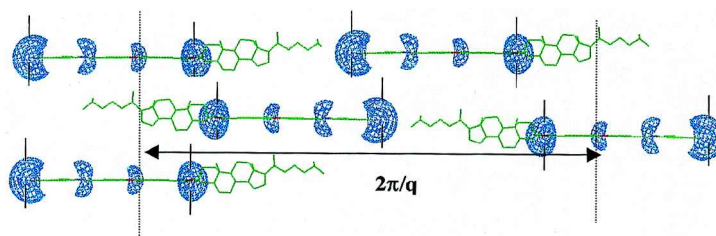

Figure 3.   Possible arrangement of the KI-5CN dimesogens.

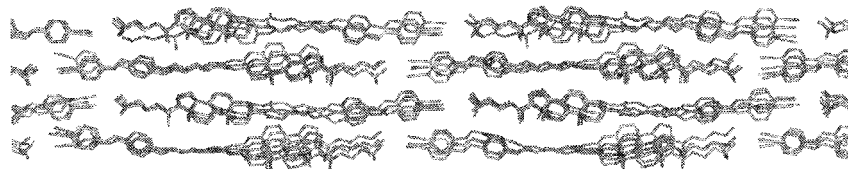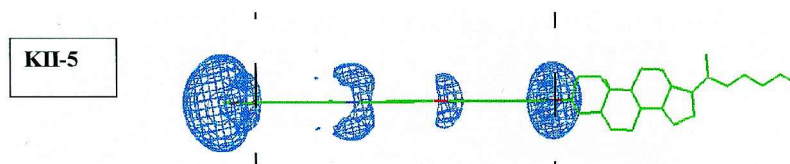Figure 4. Arrangement of the KI-5CN molecules resulting from Molecular Mechanics calculations.

Figure 5. Configuration of the KII-5 molecule.

is larger than the molecular length L, but the d/L ratio remains close to 1 ($1.01 < d/L < 1.1$). In fact, the presence of the $-C=C-$ moiety between the aromatic ring and the electron-attracting group shifts the terminal negative lobe out of the main axis of the molecule and this characteristic can impose a different overlapping of the dimesogens.

Up to now, all our investigations on non-symmetric cholesteryl dimesogens show that strict molecular conditions are required to observe simultaneously the two periodicities connected with $q1$ and to $q3$ and this explains the novelty of the incommensurate fluid smectic phases in these dimesogenic compounds.

Finally a general question is raised: is it possible to induce an incommensurate smectic phase by mixing two compounds which do not exhibit incommensurability? We will try to give an answer to this important question by discussing the binary diagram of two dimesogens, one showing an S_{q1} phase (KI-5CN) and the other an S_{q3} phase (KI-5OC$_3$). As shown in figure 6, the S_{q1} and S_{q3} smectic phases of the pure compounds are both destabilized by mixing. In a limited concentration range, anomalies of periodicity are induced in the phase diagram through the occurrence of an incommensurate smectic domain S_{ic}.

An example of the corresponding intensity profile of the X-ray diffraction pattern is given in figure 7: in the wide angle region, a broad peak centred at $(5.2 \text{Å})^{-1}$ is present indicating a low ordered smectic phase, while three incommensurate reflections are evident in the low angle region. The corresponding wave vectors $q1$, $q2$ and $q3$ appear collinear on oriented patterns. As previously observed [6], $q2$ corresponds to a satellite and the ratio of the two underlying periods $q3/q1$ is an irrational number larger than two (2.55 for the example of figure 7).
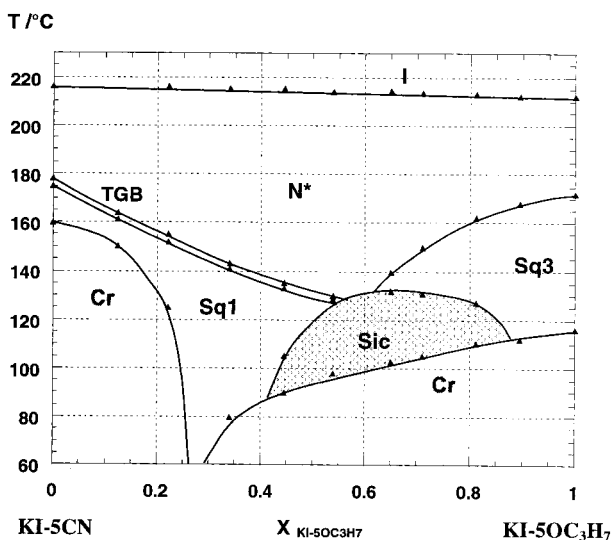

Figure 6. Isobaric temperature–concentration phase diagram for dimesogens KI-5CN (left) and KI-5OC$_3$H$_7$ (right). This phase diagram is derived from three complementary techniques: DSC, microscopic observations and X-ray analysis. The phase transitions detected by DSC correspond to small texture changes, since the S_{q1}, S_{q3} and S_{ic} phases appear very similar. Only the structural analysis allows the three phases to be characterized.
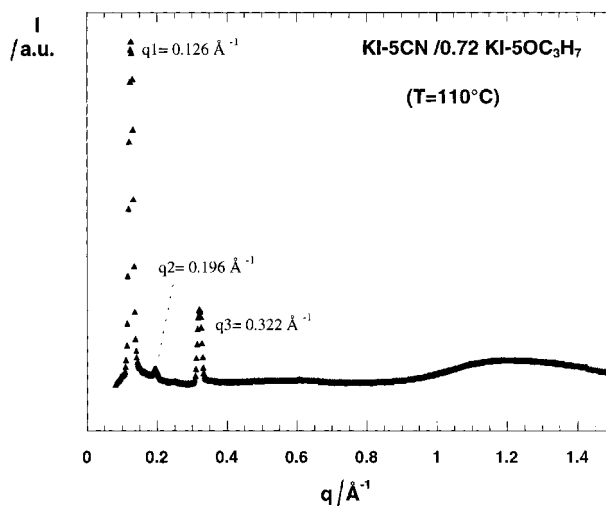

Figure 7. Intensity profile of the X-ray pattern for the KI-5CN/0.72 KI-5OC$_3$ binary mixture in the enantiotropic incommensurate domain ($T = 110°$C).
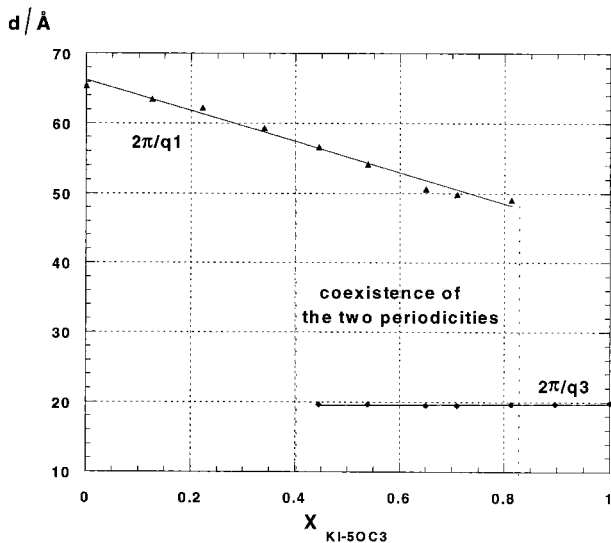
Figure 8. Evolution of the layering parameters versus composition in the KI5-CN/KI-5OC$_3$H$_7$ binary diagram.

Throughout the KI-5CN/KI-5OC$_3$H$_7$ binary diagram, the layer spacing $2\pi/q1$ decreases on increasing the KI-5OC$_3$H$_7$ content, while $2\pi/q3$ remains quasi-independent of the composition. As previously reported, this periodicity (≈ 20 Å) is imposed by the cholesteryl moiety [6]. The occurrence of anomalies of periodicity, through a two-dimensional modulated phase or an incommensurate phase, first presupposes the possibility of this $2\pi/q3$ periodicity to develop. It is clearly evident on figure 8 that the existence of the $2\pi/q3$ periodicity is limited by the value of $2\pi/q1$: the $2\pi/q3$ periodicity cannot develop when $2\pi/q1$ becomes too large, that is to say when the degree of overlapping of adjacent dimesogens is weaker. Lastly, one can recall that the S$_{q3}$ layering results from favourable interactions between the cholesteryl and the aromatic parts [2] and in this sense is prevented from forming in compounds with a strong electron-attracting terminal group, since, as shown in figure 4, the cholesteryl part interacts much more favourably with the spacer but less so with the aromatic mesogen.

References

[1] ATTARD, G. S., DATE, R. W., IMRIE, C. T., LUCKHURST, G. R., ROSKILLY, S., SEDDON, J. M., and TAYLOR, L., 1994, *Liq. Cryst.*, **16,** 529.
[2] HARDOUIN, F., ACHARD, M. F., JIN, J.-I., and YUN, Y.-K., 1995, *J. Phys. II Fr.*, **5,** 927.
[3] FAYE, V., NGUYEN, H. T., and BAROIS, P., 1997, *J. Phys. II Fr.*, **7,** 1245.
[4] HOGAN, J. L., IMRIE, C. T., and LUCKHURST, G. R., 1988, *Liq. Cryst.*, **3,** 645.
[5] SIGAUD, G., HARDOUIN, F., ACHARD, M. F., and LEVELUT, A. M., 1981, *J. Phys.*, **42,** 107.
[6] HARDOUIN, F., ACHARD, M. F., JIN, J.-I., YUN, Y.-K., and CHUNG, S. J., 1998, *Eur. Phys. J.*, **B1,** 47.
[7] HARDOUIN, F., NGUYEN, H. T., ACHARD, M. F., and LEVELUT, A. M., 1982, *J. Phys. Lett. Fr.*, **43,** L-327.
[8] HARDOUIN, F., ACHARD, M. F., JIN, J.-I., SHIN, J.-W., and YUN, Y.-K., 1994, *J. Phys. II Fr.*, **4,** 627.
[9] JIN, J.-I., 1995, *Mol. Cryst. liq. Cryst.*, **267,** 249.
[10] HARDOUIN, F., ACHARD, M. F., LAGUERRE, M., JIN, J.-I., and KO, D.-H., 1999, *Liq. Cryst.*, **26,** 589.
[11] CHA, S. W., JIN, J.-I., LAGUERRE, M., ACHARD, M. F., and HARDOUIN, F., 1999, *Liq. Cryst.*, **26,** 1325.
[12] BAROIS, P., COULON, C., and PROST, J., 1981, *J. Phys. Lett.*, **42,** L-107.
[13] HARDOUIN, F., LEVELUT, A. M., ACHARD, M. F., and SIGAUD, G., 1983, *J. Chim. Phys.,* **80,** 53 and references therein.